

Development of Lead-free Force-feedback Tactile Sensor Fabricated from BiFeO₃ Piezoelectric Film

David T. W. Lin,^{1,2} Kun-Dar Li,^{2*} Po-Chang Chen,¹ and Jia-Yun Kuo¹

¹Graduate Institute of Mechatronic System Engineering, National University of Tainan,
No. 33, Sec. 2, Shu-Lin St., West Central Dist., Tainan City 700301, Taiwan

²Department of Materials Science, National University of Tainan,
No. 33, Sec. 2, Shu-Lin St., West Central Dist., Tainan City 700301, Taiwan

(Received May 24, 2021; accepted October 1, 2021)

Keywords: tactile sensor, sol-gel, thin film, BiFeO₃

In this study, we develop a flexible lead-free BiFeO₃ (BFO) film sensor that can be applied on complex surfaces of devices. This sensor is fabricated by depositing BFO thin film on a polyimide (PI)-coated copper substrate. The sol-gel (SG) method and spin-coating method are utilized to prepare the BFO piezoelectric film. Two different spin-coating processes under three different sets of parameters and two different annealing temperatures are used in the fabrication. X-ray diffraction (XRD) and scanning electron microscopy are used to examine the crystallinity and surface topography of the BFO thin films, respectively. A lifetime test is performed on the device to validate the robustness of its piezoelectric properties, and a linear scaling relationship between the force and output response is obtained. We propose suitable conditions for preparing the piezoelectric film and demonstrate the reliability of this sensor.

1. Introduction

Wearable electronics have attracted much research attention. Special features of wearable electronics are flexibility and nontoxicity. Therefore, films and fibers have advantages over semiconductor materials in terms of cost, large scale, fabrication, and biocompatibility. These diverse substrate materials have been investigated for use in displays, memories, circuitry, photovoltaic devices, and microsensors. In this study, we fabricate a tactile sensor based on a BiFeO₃ (BFO) thin film, which is commonly used in transduction techniques as, for example, capacitive components, piezoresistors, and piezoelectric films. BFO has a crystal structure with center symmetry but no axis symmetry. This specific lattice symmetry results in piezoelectricity and pyroelectricity. BFO is also a transparent and lead-free piezoelectric material. Many investigations on BFO thin films have been reported.

In 2003, Wang *et al.* developed a BFO thin film with enhanced polarization and related properties in heteroepitaxially constrained thin films of the ferroelectromagnet BFO. Their structure analysis indicated that the crystal structure of the film was monoclinic, in contrast to the rhombohedral bulk.⁽¹⁾ There are numerous methods of preparing BFO thin films, such as the hydrothermal and coprecipitation methods, pulse laser deposition, chemical vapor deposition

*Corresponding author: e-mail: kundar@mail.nutn.edu.tw
<https://doi.org/10.18494/SAM.2021.3623>

(CVD), and the sol–gel (SG) process.^(1–4) Many researchers had reported the preparation of BFO thin films by magnetron sputtering and CVD; however, both methods are expensive. Compared with other deposition techniques, the SG technique has the advantages of low cost and low substrate temperature in the process.

In 2010, Yan *et al.* reported that only a nominal amount of pure BFO is obtained by the SG method.⁽⁵⁾ However, Bashir *et al.* reported the synthesis of pure bismuth iron oxide thin films by the SG method in 2015. The results show that by using a Bi/Fe ratio of 1.1, pure BFO can be obtained at a low temperature of 300 °C.⁽⁶⁾ Cetinkaya *et al.* prepared a pure BFO film on Si-P and glass substrates by the SG dip method in 2015.⁽⁷⁾ The capacitance–voltage ($C-V$) and conductance–voltage ($Gw-V$) electric characteristics are sensitive to applied voltage frequency. Polycrystalline BFO powder was prepared through optimized solid-state (SS) and SG reaction methods by Suresh and Srinath. The grain size of the SG-processed sample was half that of the SS-processed sample. The dielectric constant of the SG-processed sample exhibited higher values with a Maxwell–Wagner-type dielectric dispersion.⁽⁸⁾ Sharma *et al.* prepared BFO thin films with a uniform thickness of ~200 nm by a SG-assisted spin-coating method. They found that the grain size distribution become wider as the annealing temperature increased.⁽⁹⁾ In 2018, Zheng *et al.* prepared pure BFO by a microwave-assisted SG method. The synthesized BFO nanoparticles at the calcining temperature of 450 °C exhibited a rhombohedrally distorted perovskite structure without a secondary phase. The grain size decreased as the calcining temperature increased.⁽¹⁰⁾ The annealing temperature is an important factor in the film fabrication process. Ren *et al.* discussed the effect of the annealing temperature on the dielectric property in 2014.⁽¹¹⁾ Lv *et al.* proposed the modulation of the electric and magnetic properties of BFO ceramic via the annealing temperature.⁽¹²⁾ Much attention has been given to these effects of fabrication processes, such as SG and chemical solution deposition (CSD).⁽¹³⁾ Bai *et al.* also discussed the effect of the annealing temperature on BFO thin-film photoelectrodes.⁽¹⁴⁾

BFO films can be used in tactile, force-feedback applications. Ganesh *et al.* synthesized a nanocrystalline BFO powder by the SG method, followed by annealing at 100–500 °C. The fabricated piezoelectric device demonstrated an output voltage of 0.4 V upon applying the normal pressure from a human finger to the device.⁽¹⁵⁾ Yang *et al.* proposed a BFO-based dielectric capacitor and demonstrated its high energy density, superior thermal stability, and reliable bending endurance.⁽¹⁶⁾ Shi *et al.* proposed a high-frequency current sensor based on lead-free multiferroic BFO ceramic.⁽¹⁷⁾

In this study, crystalline BFO thin films are obtained and their crystallinity and surface morphology are analyzed by X-ray diffraction (XRD) and scanning electron microscopy (SEM). Additionally, force response measurement is utilized to evaluate the piezoelectric properties of the thin films. The purpose of this research is to fabricate a lead-free piezoelectric thin film that can be used in a tactile sensor to assist the diagnostic system of the computerized numerical control (CNC) machining center in the monitoring of automated processes. The piezoelectric film developed in this study can be employed in numerous fields, such as piezoelectric energy harvesters and surface acoustic wave (SAW) devices. It is hoped that the results of this study will promote the development of fabrication techniques for BFO piezoelectric films. It is difficult to obtain a stable piezoelectric effect for crystalline BFO films. With the improvement of the

fabrication parameters and lifetime tests, the fabrication of a robust lead-free BFO film sensor is proposed and verified in this study. In addition, this tactile sensor can be integrated into wireless wearable devices designed by our team.⁽¹⁸⁾

2. Fabrication

The BFO precursor solution is synthesized by dissolving $\text{Fe}(\text{NO}_3)_3 \cdot 9\text{H}_2\text{O}$, $\text{Bi}(\text{NO}_3)_3 \cdot 5\text{H}_2\text{O}$ in acetic acid and ethylene glycol with vigorous stirring for 8 h. Then, the chelating agent acetylacetonate ($\text{C}_5\text{H}_8\text{O}_2$) is added, the mixture is vigorously stirred for 12 h, and the mixture is left for 1 day to complete the reaction. Here, 10 mol% excess Bi is added to compensate the loss during the high-temperature annealing.⁽¹⁹⁾ The BFO solution is deposited on a polyimide (PI)-coated copper substrate by spin-coating to obtain a prototype piezoelectric film.

To increase the hydrophilicity and improve the adhesion of the solution on the substrate, the flexible substrate must be pretreated with atmospheric plasma. The BFO precursor solution is deposited on the substrate by spin-coating as follows. First, the specimen is coated with SG solution by spin-coating at a speed of 450 rpm for 10 or 30 s, then the speed is increased to 3000 rpm for 30 or 60 s, respectively. The coated films are baked at 250 °C for 3 min to remove the organic solvent and decrease scorching and cracking during the annealing process. Afterwards, the thin films are cured at 350 °C for 10 min. These coating and curing steps are repeated until the three layers of BFO thin film have formed. Finally, the films are annealed at 500 or 600 °C for 20 min. During the annealing process, the thin-film lattice undergoes rearrangement, eliminating the residual stress in the film. A schematic diagram and the preparation process of BFO thin film is shown in Figs. 1 and 2, respectively. The contents of the BFO solution and the preparation process are shown in Table 1 and Fig. 2, respectively. Six preparation processes are discussed for obtaining the crack-free, homogeneous crystalline BFO film; the parameters are listed in Table 2.

The crystalline quality of the film is examined by XRD at 45 kV and 40 mA with $\text{Cu K}\alpha$ radiation ($\lambda = 0.154 \text{ nm}$). The topography of the surface is observed by SEM using JEOL JSM-7600F.

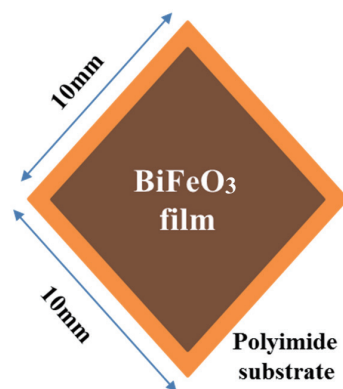


Fig. 1. (Color online) Schematic diagram of BFO thin-film tactile sensor.

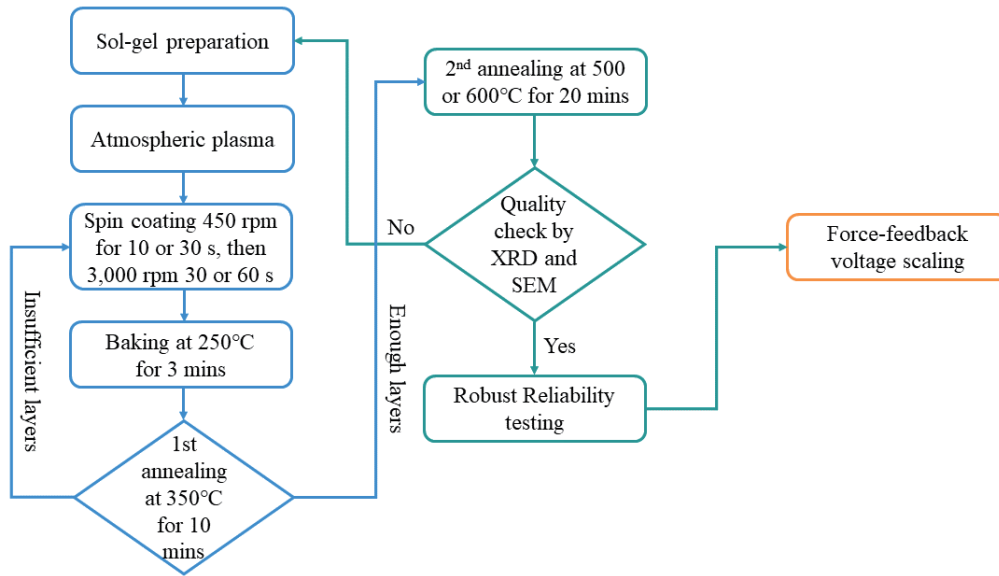


Fig. 2. (Color online) Flow chart for preparation of BFO thin-film tactile sensor.

Table 1

Contents of the BFO solution.

Iron(III) nitrate nonahydrate	0.3 mol	$\text{Fe}(\text{NO}_3)_3 \cdot 9\text{H}_2\text{O}$
Bismuth(III) nitrate	0.33 mol	$\text{Bi}(\text{NO}_3)_3 \cdot 5\text{H}_2\text{O}$
Acetic acid	15 ml	CH_3COOH
Ethylene glycol	15 ml	$\text{C}_2\text{H}_6\text{O}_2$
Acetyl acetone	30 ml	$\text{C}_5\text{H}_8\text{O}_2$

Table 2

Parameters of preparation process.

Case	Spin-coating rpm/s	Baking	1st annealing	2nd annealing
S1	450/10, 3000/30			
S2	450/30, 3000/30			500 °C/20 min
S3	450/30, 3000/60	250 °C/3 min	350 °C/10 min	
S4	450/10, 3000/30			
S5	450/30, 3000/30			600 °C/20 min
S6	450/30, 3000/60			

3. Results and Discussion

To achieve a good force-feedback response of this piezoelectric film, high crystallinity must be obtained. The parameters (listed in the Table 2) used in the film preparation are discussed.

Figures 3(a)–3(f) show SEM images of the topography of the BFO surface after the final annealing for different spin-coating conditions and annealing temperatures. The BFO particles are observed to be homogeneously dispersed when the annealing temperature is 500 °C (cases S1–S3). It is also found that the BFO film is crack-free, homogeneous, and dense when the duration of the first spin-coating is 30 s (cases S2 and S3).

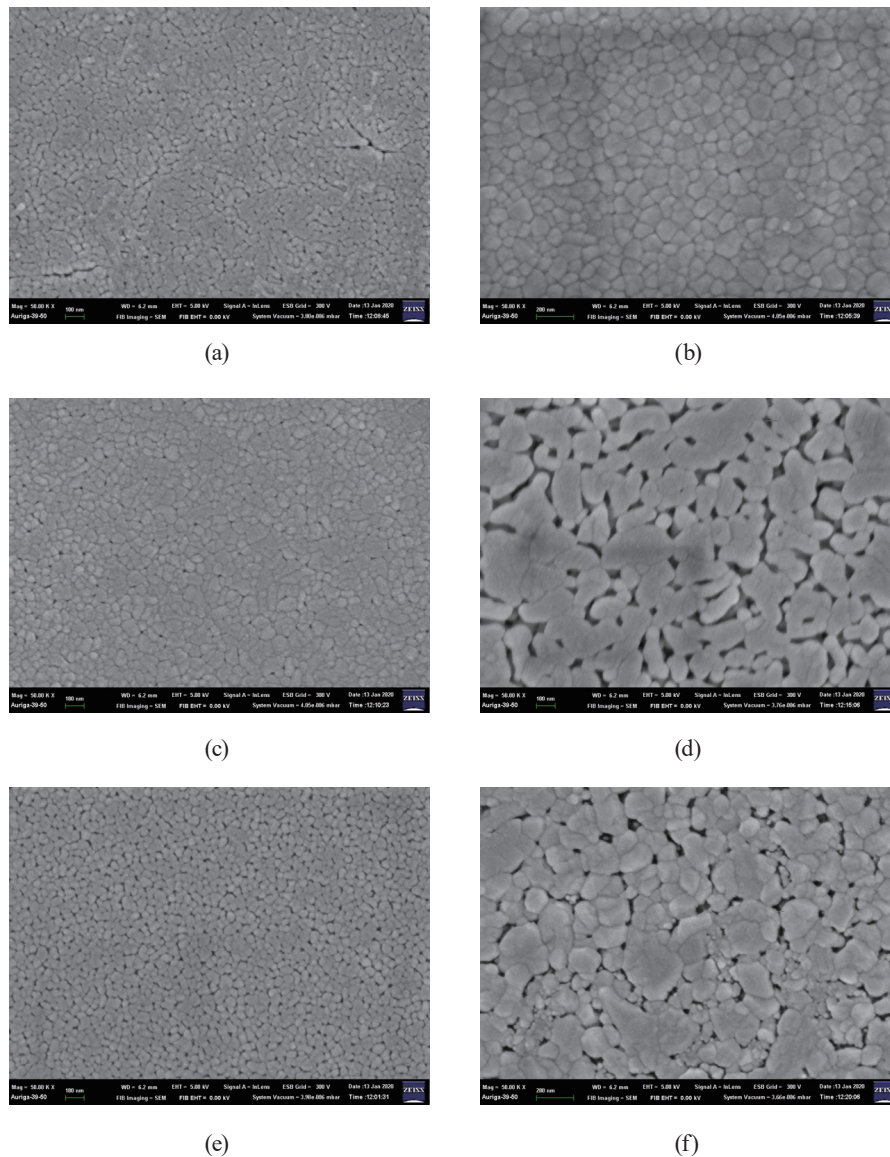


Fig. 3. (Color online) SEM images of BFO thin films: (a) S1, (b) S4, (c) S2, (d) S5, (e) S3, and (f) S6.

To demonstrate the reliability of the thin films fabricated with different parameters, the crystallinity of the layers is investigated or identified by XRD to analyze the material of the thin film. The results are shown in Fig. 4 and reveal the crystal phases of the BFO thin film under various spin-coating processes (cases S1–S3). The spectra show the diffraction peaks of (101) BFO, (021) $\text{Bi}_2\text{Fe}_4\text{O}_9$, and (310) $\text{Bi}_2\text{Fe}_4\text{O}_9$ for the BFO thin film, showing the BFO layer consists of (101) ac-axis-oriented BFO, (021) bc-axis-oriented $\text{Bi}_2\text{Fe}_4\text{O}_9$, and (310) ab-axis-oriented $\text{Bi}_2\text{Fe}_4\text{O}_9$ for all samples.

However, the peaks of (021) $\text{Bi}_2\text{Fe}_4\text{O}_9$ and (310) $\text{Bi}_2\text{Fe}_4\text{O}_9$ are impurity phases. Pure BFO is difficult to synthesize by the SG method because impurity phases such as $\text{Bi}_2\text{Fe}_4\text{O}_9$ and $\text{Bi}_{24}\text{Fe}_2\text{O}_{39}$ usually exist in BFO. The above SEM results show that the grain size of case S2 is

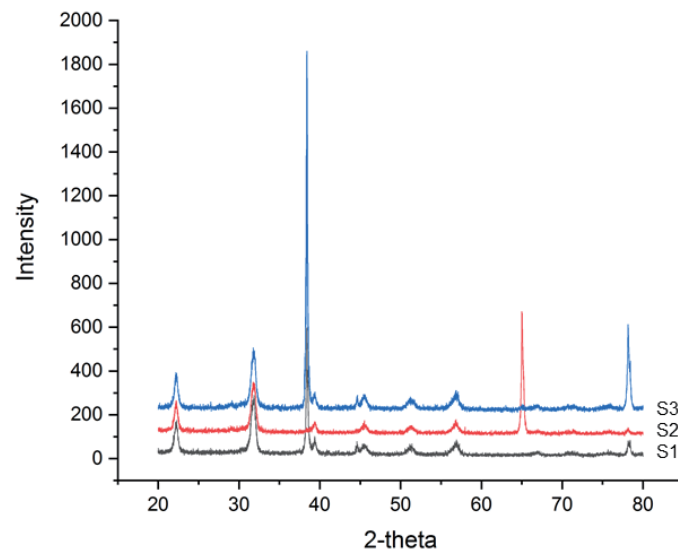


Fig. 4. (Color online) XRD spectra of BFO thin films for cases S1–S3.

close to that of case S3, and the XRD results of S2 and S3 show the BFO crystal exists. However, the intensity of the peak of pure BFO in case S3 is higher than that in case S2. Therefore, the BFO film used for subsequent testing is prepared using the parameters of case S3.

3.1 Vibration test

Three tests are adopted to investigate the performance of the tactile sensor. The first is a vibration test, where the prototype thin film is placed on a shaker with a regulated frequency and AC power amplifier. It vibrates with the assumed frequency, causing the deflection of the thin film to generate a voltage response, thus demonstrating the piezoelectric effect, as shown in Fig. 5. Figure 6 shows that the voltage response of the thin film for different frequencies. We clearly observe a stable voltage response of 0.15 V regardless of the vibrating frequency.

3.2 Lifetime test

The second test is a lifetime test, in which the above vibration is extended to 5 days, with 8 h of vibration per day, i.e., 2.88 million vibrations at 10 Hz. The voltage response is about 0.1 to 0.15 V, and the standard deviation per day is about 0.018 V, as shown in Fig. 7. This demonstrates that the BFO sensor exhibits robust and stable characteristics.

3.3 Force-feedback scaling test

Finally, the piezoelectric responses of this sensor are examined using a force-feedback testing system, as shown in Fig. 8. The output power of this sensor with different applied forces is demonstrated using this system.

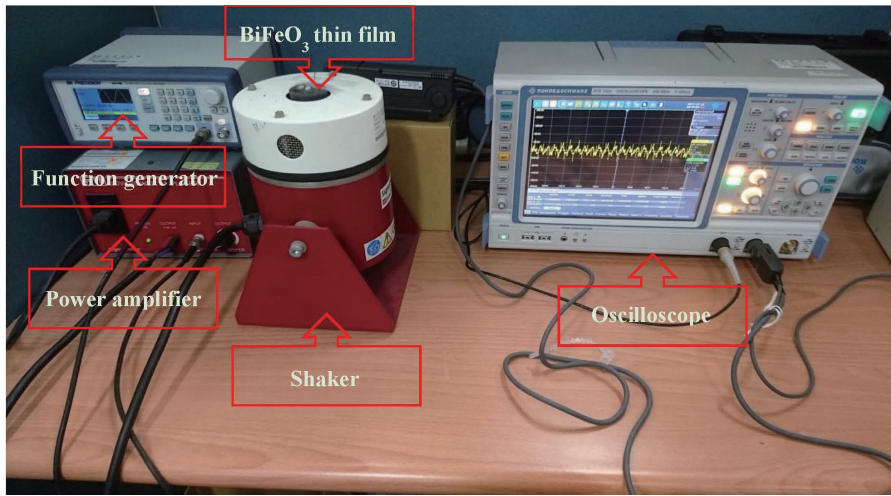


Fig. 5. (Color online) Vibration test platform.

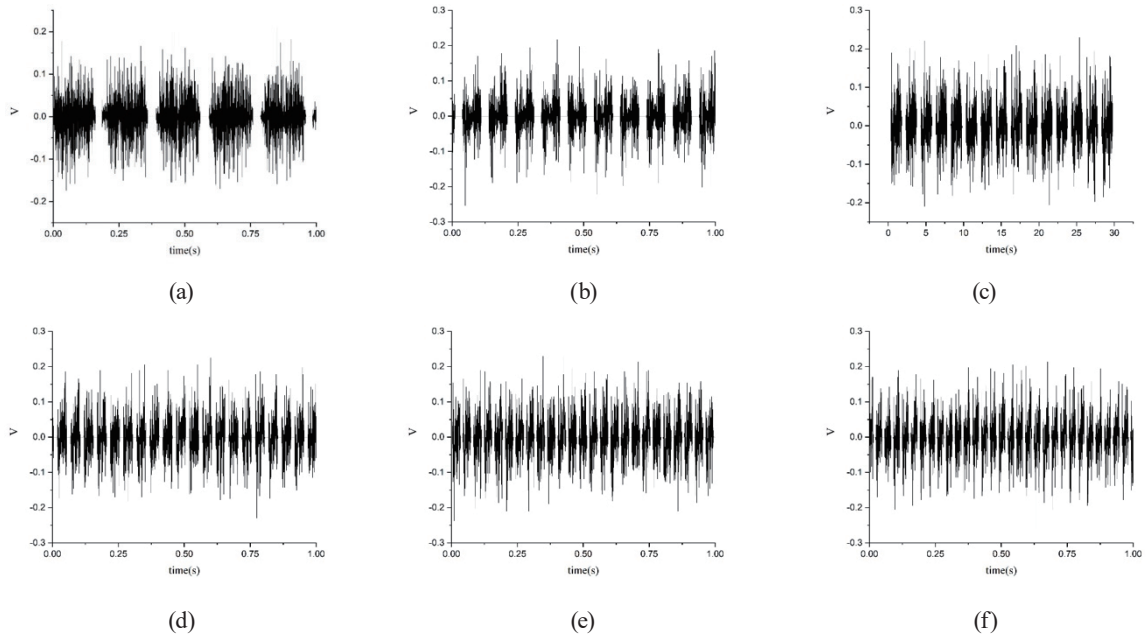


Fig. 6. Voltage response of the BFO thin film in the vibration test at frequencies of (a) 5 Hz, (b) 10 Hz, (c) 15 Hz, (d) 20 Hz, (e) 25 Hz, and (f) 30 Hz.

Figure 9 shows the force-feedback results of this sensor, which is a BFO film on a PI-coated Cu substrate; the average of five measurements is shown for each sample. The output power increases from 3.06 to 9.78 mW as the applied force increases from 10 to 40 N. It is found that the output power increases linearly with the applied force. The equation of the fitting curve is

$$y = 0.2301x + 0.675, \quad R^2 = 0.9937, \quad (1)$$

where y is the power output (mW) and x is the applied force (N).

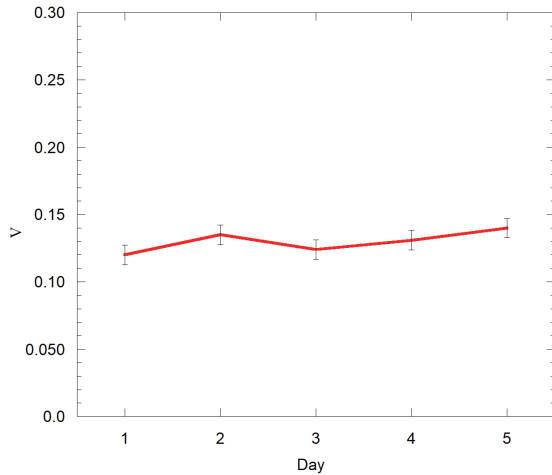


Fig. 7. (Color online) Piezoelectric response in lifetime test.

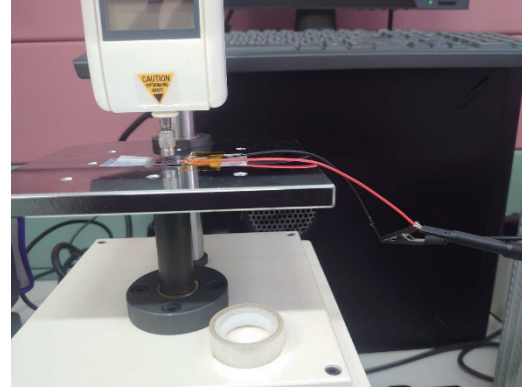


Fig. 8. (Color online) Force-feedback testing system.

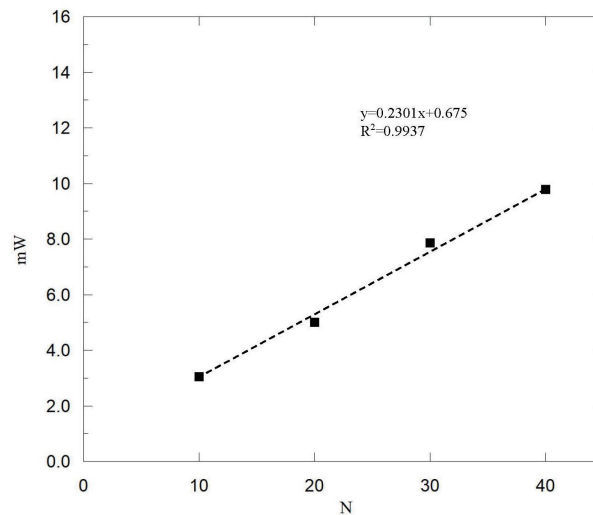


Fig. 9. Output power of BFO sensor with different applied forces.

Therefore, this sensor is verified and evaluated through the lifetime and force-feedback scaling tests, respectively. It can be used as a pressure and tactile sensor through the measurement of output power.

4. Conclusions

A flexible tactile sensor was prepared in this study. The sensor comprised a BFO thin film fabricated by the SG method that was deposited on a flexible PI-coated Cu substrate. We investigated the effects of different spin-coating and annealing temperatures on the topography of the film surface. The crystallinity of BFO was also examined by XRD. The availability and the robust response of the proposed tactile sensor were verified.

It was found from the topography of the surface and XRD spectra of the film that the best conditions for spin-coating were a first spin at 450 rpm for 30 s, followed by a second spin at

3000 rpm for 30 s, and that the most suitable annealing temperature was 500 °C. The lifetime test showed that the piezoelectric response provides a stable voltage within 0.1–0.15 V. The force-feedback test shows that the power output increases with the applied force.

The tests verified the high performance and robustness of the flexible BFO film sensor. The sensor can be used for pressure or vibration monitoring, as an energy harvester for wireless monitoring, and in the autosensing field.

Acknowledgments

The financial support provided to this study by the Ministry of Science and Technology of the Republic of China under Contract Nos. MOST 109-2221-E-024-007 and MOST 110-2221-E-024 -010 is gratefully acknowledged.

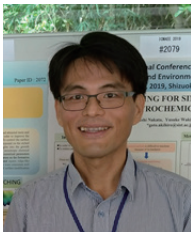
References

- 1 J. Wang, J. B. Neaton, H. Zheng, V. Nagarajan, S. B. Ogale, B. Liu, D. Viehland, V. Vaithyanathan, D. G. Schlom, U. V. Waghmare, N. A. Spaldin, K. M. Rabe, M. Wuttig, and R. Ramesh: *Science* **299** (2003) 1719. <https://doi.org/10.1126/science.1080615>
- 2 T. Tong, J. Chen, D. Jin, and J. Cheng: *Mater. Lett.* **197** (2017) 160. <https://doi.org/10.1016/j.matlet.2017.03.091>
- 3 X. Tang, J. Dai, X. Zhu, H. Lei, L. Yin, W. Song, Y. Cheng, D. Wu, and Y. Sun: *J. Magn. Mgn. Mater.* **322** (2010) 2647. <https://doi.org/10.1016/j.jmmm.2010.04.001>
- 4 Z. Lin, W. Cai, W. Jiang, C. Fu, C. Li, and Y. Song: *Ceram. Int.* **39** (2013) 8729. <https://doi.org/10.1016/j.ceramint.2013.04.058>
- 5 X. Yan, J. Chen, Y. Qi, J. Cheng, and Z. Meng: *J. Eur. Ceram. Soc.* **30** (2010) 265. <https://doi.org/10.1016/j.jeurceramsoc.2009.06.016>
- 6 S. Bashir, W. Mahmood, S. Riaz, and S. Naseem: *Mater. Today: Proc.* **2** (2015) 5373. <https://doi.org/10.1016/j.matpr.2015.11.053>
- 7 A. O. Cetinkaya, S. Kaya, A. Aktag, E. Budak, and E. Yilmaz: *Thin Solid Films* **590** (2015) 7. <https://doi.org/10.1016/j.tsf.2015.07.053>
- 8 P. Suresh and S. Srinath: *J. Alloys Compd.* **649** (2015) 843. <https://doi.org/10.1016/j.jallcom.2015.07.152>
- 9 S. Sharma, P. Saravanan, O. P. Pandey, V. T. P. Vinod, M. Černík, and P. Sharma: *J. Magn. Magn. Mater.* **401** (2016) 180. <https://doi.org/10.1016/j.jmmm.2015.10.035>
- 10 S. Zheng, J. Wang, J. Zhang, H. Ge, Z. Chen, and Y. Gao: *J. Alloys Compd.* **735** (2018) 945. <https://doi.org/10.1016/j.jallcom.2017.10.133>
- 11 Y. Ren, X. Zhu, C. Zhang, J. Zhu, J. Zhu, and D. Xiao: *Ceram. Int.* **40** (2014) 2489. <https://doi.org/10.1016/j.ceramint.2013.07.051>
- 12 J. Lv, H. Zhao, M. Wu, X. Lou, and J. Wu: *Mater. Des.* **125** (2017) 213. <https://doi.org/10.1016/j.matdes.2017.04.007>
- 13 E. B. Agustina, R. Suryana, and Y. Iriani: *Mater. Today: Proc.* **44** (2021) 3313. <https://doi.org/10.1016/j.matpr.2020.11.534>
- 14 L. Bai, X. Li, S. Wang, H. Liu, L. Shi, Q. Luo, W. Song, and D. Chen: *Int. J. Electrochem. Sci.* **16** (2021) 210721. <https://doi.org/10.20964/2021.07.25>
- 15 R. S. Ganesh, S. K. Sharma, S. Sankar, B. Divyapriya, E. Durgadevi, P. Raji, S. Ponnusamy, C. Muthamizhchelvan, Y. Hayakawa, and D. Y. Kim: *Curr. Appl. Phys.* **17** (2017) 409. <https://doi.org/10.1016/j.cap.2016.12.008>
- 16 C. Yang, J. Qian, P. Lv, H. Wu, X. Lin, K. Wang, J. Ouyang, S. Huang, X. Cheng, and Z. Cheng: *J. Mater.* **6** (2020) 200. <https://doi.org/10.1016/j.jmat.2020.01.010>
- 17 D. Shi, Q. Zhang, Y. M. Ye, L. Luo, E. K.-W. Cheng, D. Lin, and K.-H. Lam: *Measurement* **104** (2017) 287. <https://doi.org/10.1016/j.measurement.2017.03.036>
- 18 Y.-C. Du, D.T.W. Lin, C.-P. Jen, C. W. Ng, C.-Y. Chang, and Y.-X. Wen: *Sensors* **19** (2019) 507. <https://doi.org/10.3390/s19030507>
- 19 T. Y. Lei, Y. Y. Sun, H. Ren, Y. Zhang, W. Cai, and C. L. Fu: *Surf. Technol.* **43** (2014) 129. http://www.surface-techj.com/bmjs/ch/reader/create_pdf.aspx?file_no=201403025&flag=1

About the Authors



David T. W. Lin is a full professor and teaches at the Institute of Mechatronic System Engineering and the Department of Material Science, National University of Tainan, Tainan, Taiwan. He is the director of Center of Low Grade Energy, National University of Tainan. He is also on the committee of IEET and an associate editor of Journal of Chinese Society of Mechanical Engineers (SCI). He obtained a Scholarship for Excellence from the Ministry of Education (2015–2017) and Excellent Research Talent Award from the Ministry of Science and Technology (2010–2020). He has served as the chair of and been invited as the keynote speaker at many international conferences. He has published over 100 SCI, EI, and conference papers in the last five years. His research interests include film fabrication and application, energy harvesting, and energy saving. (david@mail.nutn.edu.tw)



Kun-Dar Li is a full professor at the Department of Materials Science, National University of Tainan, Tainan, Taiwan. His research interests include the modeling of materials, the characterization of material microstructures and properties, and nanostructural material fabrication. He has applied modeling and experimental methods to study radiation effects, ion implantation, thin-film deposition, and chemical etching. (kundar@mail.nutn.edu.tw)



Po-Chang Chen received his bachelor's degree from the Department of Automation and Control Engineering, Far East University, Tainan, Taiwan, in 2019 and his master's degree from the Graduate Institute of Mechatronic System Engineering, National University of Tainan, Tainan, Taiwan, in 2021. (azoroz76@gmail.com)



Jia-Yun Kuo received her bachelor's degree from the Department of Chemical Engineering at Chung Yuan Christian University, Taoyuan, Taiwan, in 2016 and her master's degree from the Graduate Institute of Mechatronic System Engineering at National University of Tainan, Tainan, Taiwan, in 2018. Since 2018, she has been a senior engineer at PlayNitride Inc., Hsinchu Science Park, Taiwan. (candice0824@gmail.com)